NMR evidence for field-induced ferromagnetism in ($Li_{0.8}$ $Fe_{0.2}$)OHFeSe superconductor

Y. P. Wu,[1,2] D. Zhao,[1,2] X. R. Lian,[3] X. F. Lu,[1,2] N. Z. Wang,[1,2] X. G. Luo,[1,2,4] X. H. Chen,[1,2,4] and T. Wu[1,2,4,*]

[1]*Hefei National Laboratory for Physical Science at Microscale and Department of Physics, University of Science and Technology of China, Hefei, Anhui 230026, People's Republic of China*

[2]*Key Laboratory of Strongly Coupled Quantum Matter Physics, University of Science and Technology of China, Chinese Academy of Sciences, Hefei 230026, People's Republic of China*

[3]*School for Gifted Young, University of Science and Technology of China, Hefei, Anhui 230026, People's Republic of China*

[4]*Collaborative Innovation Center of Advanced Microstructures, Nanjing University, Nanjing 210093, People's Republic of China*

(Received 22 September 2014; revised manuscript received 7 February 2015; published 2 March 2015)

We report on ^{7}Li and ^{77}Se nuclear magnetic resonance (NMR) measurements in the newly discovered iron-based superconductor ($Li_{0.8}$ $Fe_{0.2}$)OHFeSe. Both remarkable change in spectrum and divergence of spin-spin relaxation (T_2) are observed with decreasing temperature, suggesting a static magnetic ordering in this material. Moreover, the broadened ^{7}Li spectrum also shows a characteristic three-peak structure. Comparison of linewidth between ^{7}Li and ^{77}Se spectra indicates that there is a ferromagnetic component along the external field direction and it happens on Fe sites in the ($Li_{0.8}$ $Fe_{0.2}$)OH layer rather than the FeSe layer, which is also responsible for the three-peak structure of the ^{7}Li spectrum with ($Li_{0.8}$ $Fe_{0.2}$) random occupation. The field-dependent spectrum and T_2 suggest that the above ferromagnetic component is induced by external magnetic field. Our present results indicate that the superconductivity in ($Li_{0.8}$ $Fe_{0.2}$)OHFeSe is very robust against the observed field-induced ferromagnetism and both of them could coexist under external magnetic field.

DOI: 10.1103/PhysRevB.91.125107 PACS number(s): 74.70.Xa, 74.25.nj, 76.60.Jx

Since the discovery of high-T_c superconductivity in layered iron-based superconductors [1–4], many iron pnictide and selenide superconductors have been found and attracted wide attention [5–9]. All of them share a common FeX (X = As and Se) layered structure unit. FeSe possesses the so-called "11" structure which is the simplest structure among the iron-based superconductors. Although the T_c of bulk FeSe is only 8.0 K [7], one-unit-cell FeSe thin film on $SrTiO_3$ substrate could achieve the highest superconducting transition temperature (T_c) in iron-based superconductors with $T_c \sim 65$ K [6,10,11]. In recent years, many high-T_c FeSe-derived superconductors have also been found, such as A_x Fe_{2-y} Se_2 (A = K, Rb, Cs) and $Li_x(NH_2)_y(NH_3)_{1-y}$ Fe_2 Se_2 [12–17]. However, FeSe-derived superconductors are still very rare compared to FeAs-based superconductors. Very recently, Lu *et al.* reported a new type of FeSe-derived superconductor ($Li_{0.8}$ $Fe_{0.2}$)OHFeSe with $T_c \sim$ 43 K [18,19]. This offers a new material platform to study the underlying mechanism of superconductivity in FeSe-derived superconductors. Besides discovering superconductivity, bulk magnetization and specific heat measurements also indicate a possible magnetic order in ($Li_{0.8}$ $Fe_{0.2}$)OHFeSe below $T_m \sim$ 8.5 K [19]. Moreover, the recent first-principles calculation suggests that a novel block-checkerboard antiferromagnetism (AFM) state instead of collinear stripe AFM state may be a universal ground state for FeSe-derived superconductors, including ($Li_{0.8}$ $Fe_{0.2}$)OHFeSe [20]. How to understand the origin of magnetism in ($Li_{0.8}$ $Fe_{0.2}$)OHFeSe becomes a central issue.

In this paper, we perform ^{7}Li (92.5% abundance, $I = 3/2$) and ^{77}Se (7.5% abundance, $I = 1/2$) NMR experiments on polycrystalline $Li_{0.8}$ $Fe_{0.2}$OHFeSe samples. Both remarkable change in spectrum and divergence of spin-spin relaxation (T_2) are observed with decreasing temperature, suggesting a static magnetic ordering in this material. Moreover, such magnetism is confirmed to originate from the ($Li_{0.8}$ $Fe_{0.2}$)OH layer rather than the FeSe layer. Furthermore, a field-induced ferromagnetic behavior is also observed in present NMR experiments.

A polycrystalline sample of $Li_{0.8}$ $Fe_{0.2}$OHFeSe is synthesized by the hydrothermal reaction method with $T_c \sim 34$ K [18].The polycrystalline sample is ground and pressed into pellets to perform NMR measurement. All NMR measurements are carried out by using a commercial phase-coherent pulsed spectrometer from Thamway Company Ltd. ^{7}Li and ^{77}Se NMR spectra are obtained by integrating the spin echo intensity by sweeping NMR frequency at a fixed magnetic field of 10 T and 11 T, respectively. The spin-spin relaxation T_2 is obtained by fitting the spin echo intensity with $I(\tau) = I(0)\exp(-2\tau/T_2)$, where τ is the time separation between $\pi/2$ and π pulses. The magnetization measurements are carried out by commercial SQUID-MPMS.

First, we determine T_c under external magnetic field by measuring the temperature-dependent characteristic frequency of the circuit in an NMR probe. The initial frequency f_0 is tuned to 165.5 MHz. As shown in Fig. 1(a), the temperature-dependent characteristic frequency shows a clear transition below T_c owing to superconductivity. The Δf is obtained by subtracting nonsuperconducting background. In this way, we could obtain the H-T_c phase diagram based on the data in Fig. 1(a). As shown in Fig. 1(b), the onset temperature of the superconducting transition is used to define T_c. We find that the superconductivity in ($Li_{0.8}$ $Fe_{0.2}$)OHFeSe is very robust under high magnetic field. The T_c under zero field is determined to be about 34 K for the studied sample.

The crystal structure of ($Li_{0.8}$ $Fe_{0.2}$)OHFeSe is shown in the inset of Fig. 2 [19,21]. ^{7}Li and ^{77}Se nuclei sit in different layers, respectively. Such structural feature could be used to clarify spatial distribution of magnetism in this material. Although ^{77}Se NMR signal is not good for measurement because of the low abundance (7.5%), very low temperature measurement on

*wutao@ustc.edu.cn

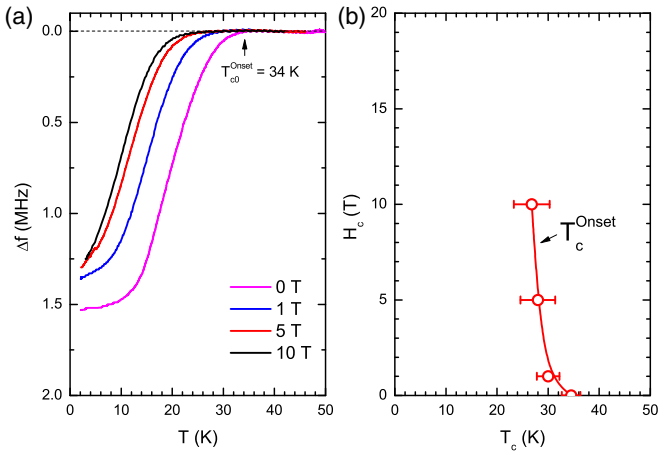

FIG. 1. (Color online) (a) Temperature-dependent relative resonance frequency of the NMR circuit [Δf(MHz)] under different external magnetic field, which is obtained by subtracting by normal-state background. (b) H-T_c phase diagram of $(Li_{0.8}Fe_{0.2})$OHFeSe; T_c is defined as the onset temperature of superconducting transition.

^{77}Se is still possible. As shown in Fig. 2, both ^{7}Li and ^{77}Se spectra at 5.5 K show a distinct broad feature. The linewidth of the ^{77}Se NMR spectrum at 5.5 K is about 4 MHz (~0.4 T internal field distribution), which is almost two orders of magnitude bigger than that in nonmagnetic FeSe [22], suggesting a static magnetic ordering in this material. Such broad spectrum makes the measurement at high temperature impossible with ^{77}Se nuclei. Compared with the ^{77}Se NMR spectrum, the ^{7}Li NMR spectrum is even broader and shows a three-peak structure. It is worth reminding that a similar broad spectrum is also observed in another FeSe-derived superconductor, $Rb_x Fe_{2-y} Se_2$ [23]. In that case, another narrow peak could be also observed in

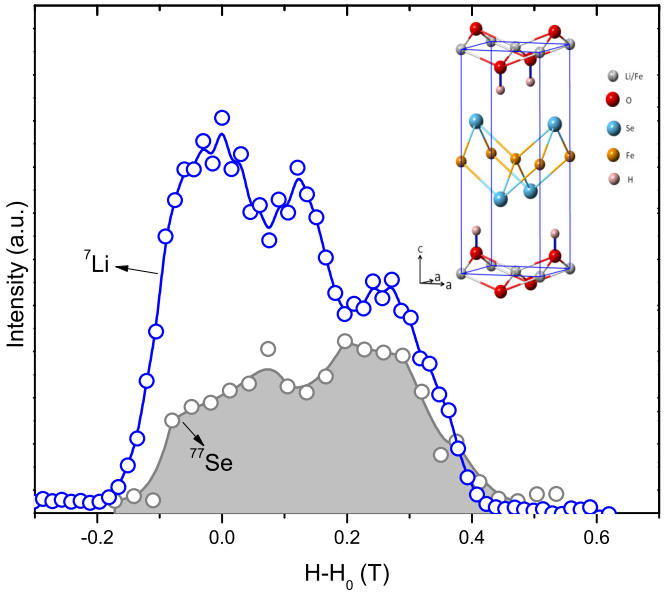

FIG. 2. (Color online) ^{7}Li and ^{77}Se NMR spectra at 5.5 K under external magnetic field $H_0 = 11$ T and 10 T, respectively. The inset shows the crystalline structure of $(Li_{0.8}Fe_{0.2})$OHFeSe determined by neutron scattering [19,21].

$Rb_x Fe_{2-y} Se_2$, which is ascribed to phase separation of SC and AFM domains. We did not observe such phase separation feature in our experiment, suggesting a spatial uniform magnetism in $(Li_{0.8}Fe_{0.2})$OHFeSe. Our results indicate that both ^{7}Li and ^{77}Se feel a broad internal field distribution due to emergence of a static magnetic ordering at 5.5 K. Such static magnetic ordering may originate from the $(Li_{0.8}Fe_{0.2})$OH layer or FeSe layer. If we consider magnetism from the FeSe layer, the ^{77}Se should feel a much broader internal field distribution than that of ^{7}Li by dipolar field calculation. Similar conclusion is also obtained in the case of $Rb_x Fe_{2-y} Se_2$ [23], in which AFM is located in the FeSe layer and ^{77}Se hyperfine coupling to Fe spins is twice as large as that of ^{87}Rb. Therefore, our results exclude that the observed magnetism happens in the FeSe layer. The only choice for the location of magnetism should be on Fe sites in the $(Li_{0.8}Fe_{0.2})$OH layer. In the following context, considering the magnetism in the $(Li_{0.8}Fe_{0.2})$OH layer with a ferromagnetic component along the external field direction, we could confirm that the three-peak structure in the ^{7}Li spectrum is caused by random occupation between Fe and Li ions in the $(Li_{0.8}Fe_{0.2})$OH layer.

As shown in Fig. 3, the temperature-dependent ^{7}Li spectrum shows a distinct broad feature as temperature decreases below 20 K. The high-temperature ^{7}Li spectrum is symmetric around zero internal field, which corresponds to a paramagnetic normal state. Since ^{7}Li has nuclear spin $I = 3/2$ and is located in a non-cubic-symmetry environment, the corresponding electric field gradient (EFG) tensor and Knight shift tensor should give anisotropic NMR spectra. Although a polycrystalline sample is used here, there is no observable anisotropic effect in the present spectrum. This means that the anisotropic effect is masked by broadening effect of linewidth. This would simplify our discussion below. As the temperature decreases below 20 K, there is an additional spectrum weight that appears on the positive internal field side but not for the negative side. This change turns the whole spectrum shape into a three-peak structure with different positive internal field shift for each peak. This phenomenon indicates that a static magnetic ordering happens and creates different internal fields on ^{7}Li sites. We mark the three peaks by Li(0), Li(1), and Li(2) as shown in Fig. 3(b). In order to explain these different ^{7}Li sites, we consider a ferromagnetic component along the external field direction on each Fe site with local magnetic moment m_0 in the $(Li_{0.8}Fe_{0.2})$OH layer. In general, the internal field at nonmagnetic irons could contain two kinds of contribution through the transferred hyperfine coupling and dipolar coupling to magnetic irons. It could be expressed as $\vec{H}_{\rm loc} = \sum_j A_{hf}\vec{m}_j + \sum_j \{\frac{3(\vec{m}_j\cdot\vec{r}_j)\vec{r}_j}{r_j^5} - \frac{\vec{m}_j}{r_j^3}\}$, where A_{hf} is the transferred hyperfine coupling constant, $\vec{m}_j$ is the magnetic moment at the jth Fe site, and $\vec{r}_j$ is the vector connecting the Li site to the jth Fe site. We find that only considering the dipolar term cannot reproduce the observed internal field distribution, especially for the three-peak structure. Therefore, we suggest that the transferred hyperfine coupling to the nearest-neighboring (NN) Fe site in the $(Li_{0.8}Fe_{0.2})$OH layer should be responsible for such three-peak structure through the Fe-O-Li orbital mixing, which gives a positive internal field on Li sites. Because of the random distribution of Li and Fe ions in the $(Li_{0.8}Fe_{0.2})$OH layer, we assume the Li(0), Li(1), and

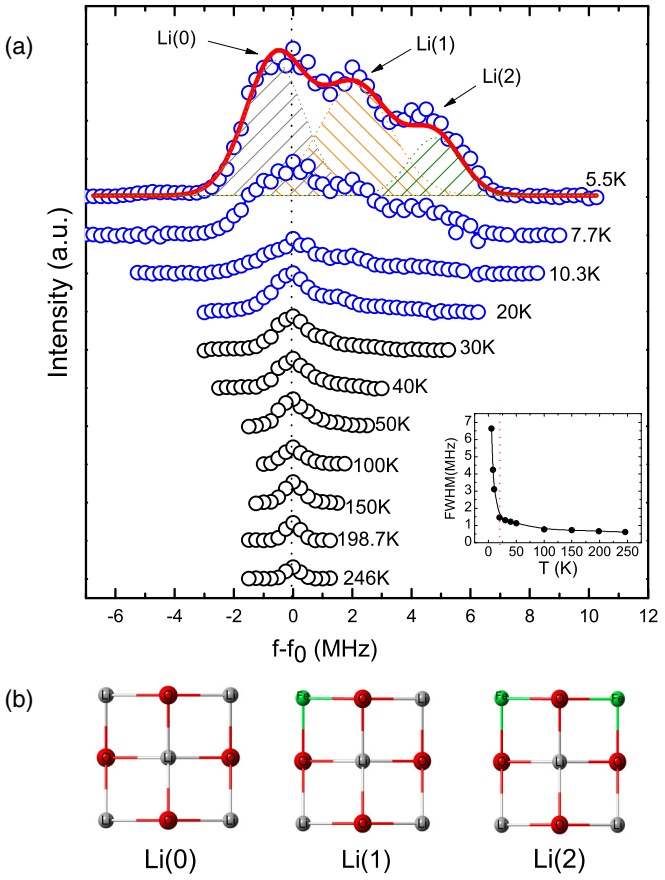

FIG. 3. (Color online) (a) Temperature-dependent ^{7}Li spectra under external magnetic field $H = 10$ T. The three peaks appearing at 5.5 K are marked by Li(0), Li(1), and Li(2), respectively. The red solid line in 5.5 K spectrum is fitted by three Gaussian peaks with fixed area ratio (details in the main text). The inset plot shows temperature dependence of the full width at the half maximum (FWHM) of the corresponding ^{7}Li spectra. (b) Three possible configurations for Li sites: Li(0), Li(1), and Li(2). Fe, Li, and O atoms are shown with green, gray, and red colors, respectively.

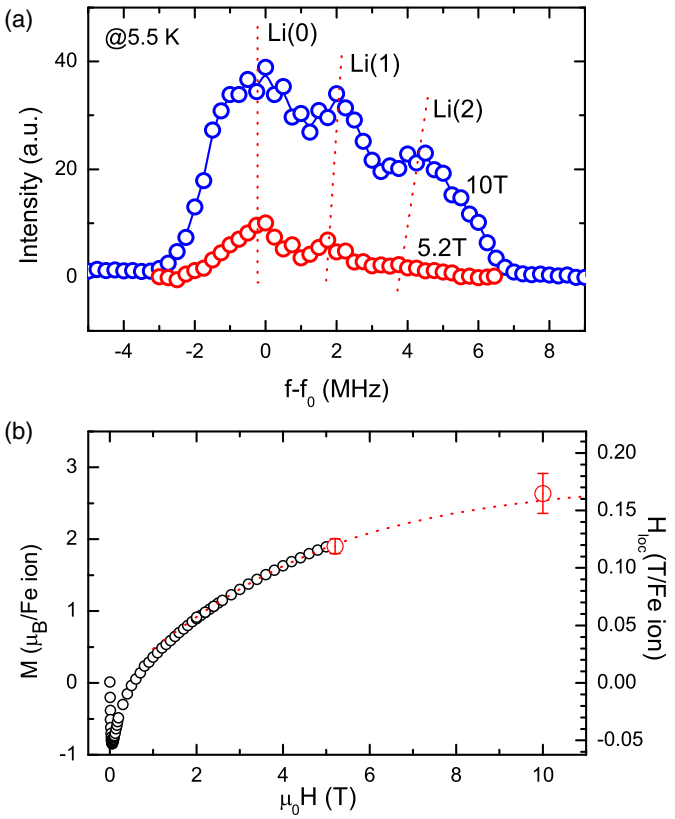

FIG. 4. (Color online) (a) Field-dependent ^{7}Li spectra at $T = 5.5$ K. The red dashed lines show the shift of Li(0), Li(1), and Li(2) sites with decreasing magnetic field. (b) Relation between bulk magnetization and local magnetization. The M-H curve at 5 K is shown by black circles. The high-field part of the M-H curve (>5 T) as shown by red dashed line is obtained by extrapolating the low-field part with Brillouin function $M = gJ\mu_B B_J(x)$, where $B_J(x)$ is Brillouin function and $x = \frac{g\mu_B J}{k_B T}\mu_0 H$. The Brillouin function gives a good fitting for magnetization data above 2 T and starts to deviate below 2 T due to superconducting signal. Red circles are the internal fields at Li sites transferred by each NN Fe ion under $H = 5.2$ T and 10 T.

Li(2) sites correspond to Li sites with 0, 1, and 2 NN Fe ions. In this case, the internal field $H(i)$ for different Li sites should be equal to $A_{hf} \times i \times m_0$ ($i = 0, 1, 2$), which is quite consistent with our observed results. Considering 20% occupation ratio of Fe, their corresponding probability should be $P_0 = 0.4096$, $P_1 = 0.4096$, and $P_2 = 0.1536$, respectively(probability for 3 and 4 NN Fe ions is negligible). As shown in Fig. 3(a), we can fit the low-temperature ^{7}Li spectrum well by using three Gaussian peaks with fixed area ratio $A_0 : A_1 : A_2 = P_0 : P_1 : P_2$. Each NN Fe ion gives an internal field shift about 1.65 kOe on the Li site estimated from the above analysis of the ^{7}Li spectrum. Furthermore, we also studied the field dependence of the observed ferromagnetic components. As shown in Fig. 4(a), the separation in three-peak structure becomes larger with increasing external field from 5.2 T to 10 T. This means that the hyperfine field created by NN Fe ions is enhanced as increasing external field. This enhancement is consistent with the M-H curve in bulk magnetization measurement as shown in Fig. 4(b), suggesting a field-induced ferromagnetic component at Fe ions. Using the bulk magnetization and internal field estimated from the ^{7}Li NMR spectrum, we could estimate the effective hyperfine coupling constant $A_{hf} \sim 0.06$ T/μ_B for each NN Fe ion. Here, if we consider that the dipole field would partly compensate the transferred hyperfine field, the actual transferred hyperfine coupling constant would be slightly bigger than the above value.

In order to further understand the field-induced ferromagnetic behavior, the temperature-dependent T_2 of ^{7}Li is also studied. T_2 measurement is carried out on the central frequency of Li(0) sites under $H = 5.2$ and 10 T, respectively. As shown in Fig. 5, temperature-dependent T_2 shows a temperature-independent behavior above 20 K and becomes divergent at the low-temperature region, where the three-peak structure appears in the spectrum. Such divergence of T_2 is ascribed to the appearance of static magnetic ordering at low temperature. As the external magnetic field decreases, the above divergence becomes weaker, which is consistent with a field-induced magnetism. We also tried to measure spin-lattice relaxation (T_1) for ^{7}Li nuclei. However, the T_1 is very short (<1 ms) in the whole temperature range.

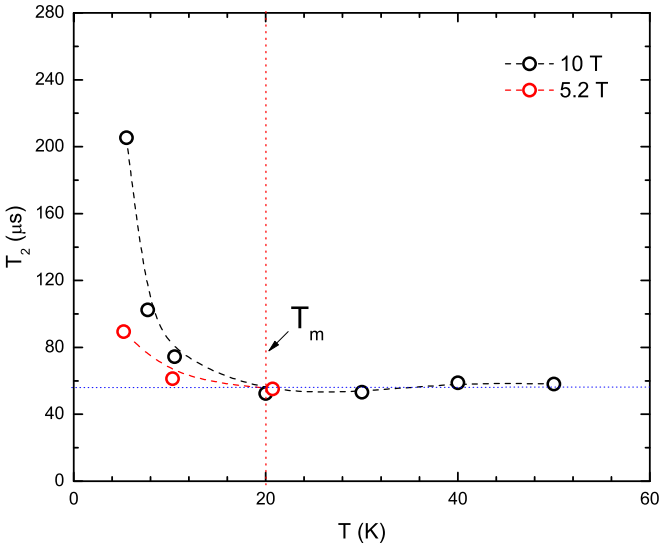

FIG. 5. (Color online) Temperature-dependent T_2 of Li(0) sites under external magnetic field $H = 10$ T (black) and 5.2 T (red), respectively. The different T_2 values compared to earlier work are caused by adopting a different prefactor in the T_2 decay formula [19], which does not change the temperature dependence of T_2 and relevant conclusions.

In the crystalline structure as shown in Fig. 2, Li and Fe irons randomly occupy the same sites in the $(Li_{0.8}Fe_{0.2})$OH layer and only Fe ions are magnetic. In this case, the $(Li_{0.8}Fe_{0.2})$OH layer could be treated as a diluted magnetic lattice. In a diluted magnetic system, the effective magnetic interaction between magnetic atoms is much reduced compared to systems without magnetic dilution. The estimated transferred hyperfine coupling between nearest-neighboring Li and Fe irons from our NMR result is quite small, which supports a much weaker magnetic interaction between magnetic Fe ions in the $(Li_{0.8}Fe_{0.2})$OH layer. On the other hand, the magnetic coupling between neighboring $(Li_{0.8}Fe_{0.2})$OH layers should be also very important for the magnetism at Fe sites in the $(Li_{0.8}Fe_{0.2})$OH layer. Such interlayer coupling is mediated by the FeSe layer and would be also very weak considering the large distance between neighboring $(Li_{0.8}Fe_{0.2})$OH layers. In previous specific heat measurements, a peak below 8.5 K was observed under zero field [19]. Furthermore, the peak temperature was found to be field-independent and this was ascribed to the existence of antiferromagnetism at zero field [19]. Considering that both interlayer and intralayer magnetic couplings between Fe ions in $(Li_{0.8}Fe_{0.2})$OH layers are very weak, the above antiferromagnetism at zero field would be very fragile under external magnetic field. Under strong external magnetic field, such antiferromagnetism could be easily altered and a ferromagnetic component along field direction is also expected. Our present NMR results under strong magnetic field indicate that the antiferromagnetism at zero field is indeed very fragile and a field-induced ferromagnetic component appears with external magnetic field which is also consistent with previous specific heat results [19]. Similar field-induced ferromagnetism is also observed in $EuFe_2As_2$ [24]. Although a novel block-checkerboard AFM state has been proposed to be a ground state for FeSe-derived superconductors [20], we did not find any trace of such a phase in the present $(Li_{0.8}Fe_{0.2})$OHFeSe superconductor. Considering the high-field superconducting transition observed in Fig. 1, we propose that superconductivity in the FeSe layer is very robust against the above field-induced ferromagnetism in the $(Li_{0.8}Fe_{0.2})$OH layer and both of them could coexist under external magnetic field for this newly discovered FeSe-derived superconductor. Although there is a field-induced ferromagnetism under external magnetic field, superconductivity coexists with antiferromagnetism at zero field in $(Li_{0.8}Fe_{0.2})$OHFeSe. How to understand the interplay between superconductivity and magnetism in this FeSe-derived superconductor needs more investigations. This would be helpful to understand the role of magnetism on the mechanism of high-T_c superconductivity.

To summarize, we perform a site-selective NMR experiment on polycrystalline $(Li_{0.8}Fe_{0.2})$OHFeSe. Our results indicate that a static magnetic ordering appears in the $(Li_{0.8}Fe_{0.2})$OH layer as temperature decreases. Moreover, such magnetic ordering possesses a field-induced ferromagnetic component along the external field direction. Our present results indicate that the superconductivity in $(Li_{0.8}Fe_{0.2})$OHFeSe is very robust against the observed field-induced ferromagnetism and both of them could coexist under external magnetic field. This also offers a new platform to study the interplay between superconductivity and magnetism.

Note added. Recently we noticed a paper [25] reporting a similar ^{7}Li NMR result but at lower field.

This work is supported by the National Natural Science Foundation of China (Grant No. 11374281), the "Strategic Priority Research Program (B)" of the Chinese Academy of Sciences (Grant No. XDB04040100), the National Basic Research Program of China (973 Program, Grant No. 2012CB922002). Specialized Research Fund for the Doctoral Program of Higher Education (Grant No. 20133402110032), the Recruitment Program of Global Experts, and the CAS Hundred Talents Program.

[1] Y. Kamihara, T. Watanabe, M. Hirano, and H. Hosono, J. Am. Chem. Soc. **130**, 3296 (2008).
[2] X. H. Chen, T. Wu, G. Wu, R. H. Liu, H. Chen, and D. F. Fang, Nature (London) **453**, 761 (2008).
[3] G. F. Chen, Z. Li, D. Wu, G. Li, W. Z. Hu, J. Dong, P. Zheng, J. L. Luo, and N. L. Wang, Phys. Rev. Lett. **100**, 247002 (2008).
[4] Z.-A. Ren, W. Lu, J. Yang, W. Yi, X.-L. Shen, Z.-C. Li, G.-C. Che, X.-L. Dong, L.-L. Sun, F. Zhou, and Z.-X. Zhao, Chin. Phys. Lett. **25**, 2215 (2008).
[5] M. Rotter, M. Tegel, and D. Johrendt, Phys. Rev. Lett. **101**, 107006 (2008).
[6] X. C. Wang, Q. Liu, Y. Lv, W. Gao, L. X. Yang, R. C. Yu, F. Y. Li, and C. Jin, Solid. State. Commun. **148**, 538 (2008).

[7] F. C. Hsu, J. Y. Luo, K. W. Yeh, T. K. Chen, T. W. Huang, P. M. Wu, Y. C. Lee, Y. L. Huang, Y. Y. Chu, D. C. Yan, and M. K. Wu, Proc. Natl. Acad. Sci. USA **105**, 14262 (2008).

[8] Q. Y. Wang, Z. Li, W. H. Zhang, Z. C. Zhang, J. S. Zhang, W. Li, H. Ding, Y. B. Ou, P. Deng, K. Chang, J. Wen, C. L. Song, K. He, J. F. Jia, S. H. Ji, Y. Y. Wang, L. L. Wang, X. Chen, X. C. Ma, and Q. K. Xue, Chin. Phys. Lett. **29**, 037402 (2012).

[9] X. H. Chen, P. C. Dai, D. L. Feng, T. Xiang, and F.-C. Zhang, Natl. Sci. Rev. **1**, 371 (2014).

[10] D. F. Liu, W. H. Zhang, D. X. Mou, J. F. He, Y. B. Ou, Q. Y. Wang, Z. Li, L. L. Wang, L. Zhao, S. L. He, Y. Y. Peng, X. Liu, C. Y. Chen, L. Yu, G. D. Liu, X. L. Dong, J. Zhang, C. T. Chen, Z. Y. Xu, J. P. Hu, X. Chen, X. C. Ma, Q. K. Xue, and X. J. Zhou, Nat. Commun. **3**, 931 (2012).

[11] S. L. He, J. F. He, W. H. Zhang, L. Zhao, D. F. Liu, X. Liu, D. X. Mou, Y. B. Ou, Q. Y. Wang, Z. Li, L. L. Wang, Y. Y. Peng, Y. Liu, C. Y. Chen, L. Yu, G. D. Liu, X. L. Dong, J. Zhang, C. T. Chen, Z. Y. Xu, X. Chen, X. C. Ma, Q. K. Xue, and X. J. Zhou, Nat. Mater. **12**, 605 (2012).

[12] J. G. Guo, S. F. Jin, G. Wang, S. C. Wang, K. X. Zhu, T. T. Zhou, M. He, and X. L. Chen, Phys. Rev. B **82**, 180520(R) (2010).

[13] A. F. Wang, J. J. Ying, Y. J. Yan, R. H. Liu, X. G. Luo, Z. Y. Li, X. F. Wang, M. Zhang, G. J. Ye, P. Cheng, Z. J. Xiang, and X. H. Chen, Phys. Rev. B **83**, 060512(R) (2011).

[14] A. Krzton-Maziopa, Z. Shermadini, E. Pomjakushina, V. Pomjakushin, M. Bendele, A. Amato, R. Khasanov, H. Luetkens, and K. Conder, J. Phys.: Condens. Matter **23**, 052203 (2011).

[15] T. P. Ying, X. L. Chen, G. Wang, S. F. Jin, T. T. Zhou, X. F. Lai, H. Zhang, and W. Y. Wang, Sci. Rep. **2**, 426 (2012).

[16] A. Krzton-Maziopa, E. V. Pomjakushina, V. Yu Pomjakushin, F. von Rohr, A. Schilling, and K. Conder, J. Phys.: Condens. Matter **24**, 382202 (2012).

[17] M. Burrard-Lucas, D. G. Free, S. J. Sedlmaier, J. D. Wright, S. J. Cassidy, Y. Hara, A. J. Corkett, T. Lancaster, P. J. Baker, S. J. Blundell, and S. J. Clarke, Nat. Mater. **12**, 15 (2013).

[18] X. F. Lu, N. Z. Wang, G. H. Zhang, X. G. Luo, Z. M. Ma, B. Lei, F. Q. Huang, and X. H. Chen, Phys. Rev. B **89**, 020507(R) (2014).

[19] X. F. Lu, N. Z. Wang, H. Wu, Y. P. Wu, D. Zhao, X. Z. Zeng, X. G. Luo, T. Wu, W. Bao, G. H. Zhang, F. Q. Huang, Q. Z. Huang, and X. H. Chen, Nat. Mater. **14**, 325 (2015).

[20] H. Y. Cao, S. Y. Chen, H. J. Xiang, and X. G. Gong, Phys. Rev. B **91**, 020504 (2015).

[21] H. L. Sun, D. N. Woodruff, S. J. Cassidy, G. M. Allcroft, S. J. Sedlmaier, A. L. Thompson, P. A. Bingham, S. D. Forder, S. Cartenet, N. Mary, S. Ramos, F. R. Foronda, B. H. Williams, X. D. Li, S. J. Blundell, and S. J. Clarke, Inorg. Chem. **54**, 1958 (2015).

[22] T. Imai, K. Ahilan, F. L. Ning, T. M. McQueen, and R. J. Cava, Phys. Rev. Lett. **102**, 177005 (2009).

[23] Y. Texier, J. Deisenhofer, V. Tsurkan, A. Loidl, D. S. Inosov, G. Friemel, and J. Bobroff, Phys. Rev. Lett. **108**, 237002 (2012).

[24] T. Wu, G. Wu, H. Chen, Y. L. Xie, R. H. Liu, X. F. Wang, and X. H. Chen, J. Magn. Magn. Mater. **321**, 3870 (2009).

[25] U. Pachmayr, F. Nitsche, H. Luetkens, S. Kamusella, F. Brückner, R. Sarkar, H.-H. Klauss, and D. Johrendt, Angew. Chem., Int. Ed. **54**, 293 (2015).